

STUDY OF THE EFFECT OF MULTIPOLAR COMPONENTS IN THE SPARC EMITTANCE COMPENSATION GUN SOLENOID*

M. Ferrario, M. Migliorati, P. Musumeci, L. Palumbo, M. Preger, C. Sanelli,
INFN-LNF, Frascati (Roma),Italy,

G. Dattoli, L. Picardi, M. Quattromini, C. Ronsivalle, ENEA-CR, Frascati(Roma), Italy
J. Rosenzweig, UCLA, Los Angeles(CA),USA, G. Bazzano, CNAO Foundation (Milano), Italy

Abstract

The SPARC photoinjector rf gun requires a solenoid immediately downstream for emittance compensation. The analysis of the measured solenoid magnetic maps shows the existence of multipolar components added to the pure solenoid field.

The effect of these added fields on beam dynamics and possible correction schemes have been studied from the theoretical point of view and by numerical calculations based on PARMELA/TREDI codes. An accurate 3D numerical modelization by using CST EM Studio has been done, in order to investigate the source of these multipolar components and to suggest some design modifications aimed to reduce their magnitude. The results of this study are presented here.

THE SPARC SOLENOID

The SPARC project, based on a collaboration among ENEA-INFN-CNR-Universita` di Roma Tor Vergata-INFM-ST, consists in a high brightness photoinjector driving FEL experiments using SASE, seeding and non-linear resonant harmonics [1].

The photocathode RF gun is followed by a solenoid immediately downstream for proper emittance compensation. The SPARC solenoid (Fig. 1) was designed to be similar to the standard BNL/LCLS type of device. Like previous versions, it employs field stiffening iron between coil sections, but uses only four coils that are independently powered, in order to shape the field profile with the aim to optimize the emittance compensation process.

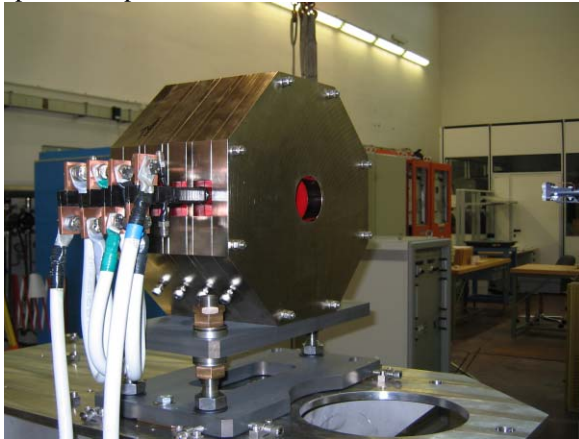


Figure 1: The SPARC emittance compensating solenoid

Magnetic measurements analysis

The axial component of the magnetic field $B_z(x,y,z)$ was scanned by an Hall probe. The scan was performed on a length on the z axis of 70 cm with a step size of 10 mm in a transverse grid defined by $-10 \text{ mm} < x, y < 10 \text{ mm}$ with a step size of 5 mm.

In order to extract the B_x and B_y components accordingly with the Maxwell equations in the beam region we did a conditioned bi-dimensional least square fit of the measured values of B_z up to the second order in x, y :

$$B_z = b_0(z) + b_1(z)x + b_2(z)y + b_3(z)x^2 + b_4(z)y^2 \quad (1)$$

with

$$b_0(z) = B_z(x = y = 0)$$

$$b_3(z) = -b_0(z)'' / 4 + \delta(z)$$

$$b_4(z) = -b_0(z)'' / 4 - \delta(z)$$

The conditions imposed on the coefficients b_0, b_3, b_4 allow to satisfy $\text{div} \vec{B} = 0$ near the axis [2].

For a pure solenoid $b_1 = b_2 = 0$ (no dipolar terms), $\delta = 0$ (no skew quadrupolar terms).

Finally the transverse components B_x and B_y were retrieved from B_z accordingly with $\text{curl} \vec{B} = 0$.

From this analysis carried on the measured map at the operating current of 140 A b_1, b_2 and δ result different from zero: b_1 and b_2 correspond to dipolar fields of the order of 10 gauss, while the longitudinal integral of δ gives a skew quadrupole with a focal length at 5.6 MeV of about 10 m. These spurious fields retrieved in such way are shown in figure 2.

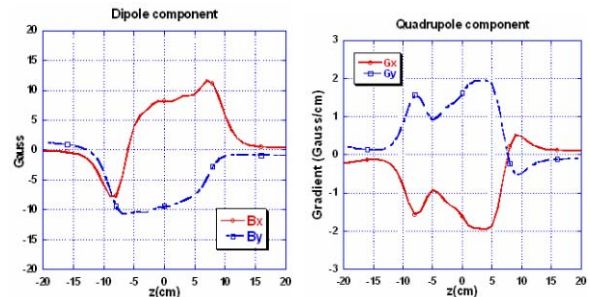


Figure 2 Added fields to the SPARC solenoid retrieved by the analysis of the longitudinal field measured map

*Work supported by EUROFEL

3D model

One of the possible sources of the quadrupolar component has been found by performing very accurate 3D computations (with 5 million of meshcells) based on CST EM Studio code.

The multipolar content has been computed by a Fourier analysis of the field on a $r_{ref}=1$ cm radius at different z positions accordingly with

$$B_{\theta}(r = r_{ref}) = \sum_{n=1}^8 [a_n \cdot \cos(n\theta) + b_n \cdot \sin(n\theta)] \quad (2)$$

with a_n =amplitudes of normal multipoles, b_n =amplitude of skew multipoles.

The comparison between the iron geometries shown in figure 3 put in evidence the presence of a skew quadrupolar component of the same order of magnitude of the measured one located in the fringing fields region of the SPARC magnet due to the lack of holes in the top and bottom of the iron shield.

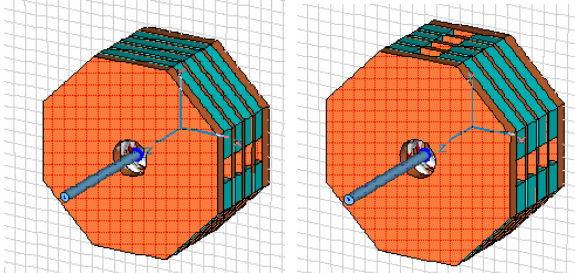


Figure 3: (Left) SPARC magnet geometry: not quadrupole compensated iron geometry, (Right) quadrupole compensated iron geometry

This is shown in figure 4, where the computed normal and skew components up to the octupole are plotted for the two compared geometries. One can see that in a symmetrized geometry a weak skew octupole appears. Other effects given by misalignments or real coils geometry have not been taken into account.

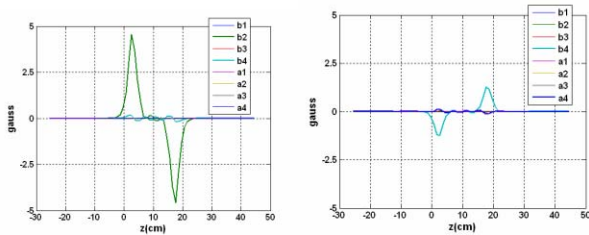


Figure 4: (Left) Multipole content in the SPARC geometry (Right) Multipole content in a quadrupole compensated iron geometry

EFFECT ON BEAM DYNAMICS

The effect of the multipolar components on the beam evolution in the post-gun drift region has been evaluated by numerical computations and a semi-analytical model. In the beam dynamics calculations we used a 3D magnetic field map built starting from the measurement of the only longitudinal component of the field accordingly with the method described above. In this way

it was possible to separate the effect of the dipolar and quadrupolar components by putting $\delta=0$ (only dipolar components) or $b_1=b_2=0$ (only quadrupolar component) in the magnetic field expansion of equation (1).

The results are shown in figures 5,6; the dipolar component essentially is a steerer, acting in different ways in the two transverse planes accordingly with the different shapes of B_x and B_y on the axis (see fig.2). As to the skew quadrupolar component, it transforms the initial round beam into an elliptical beam and gives a projected emittance growth of a factor 1.7 respect to the ideal case.

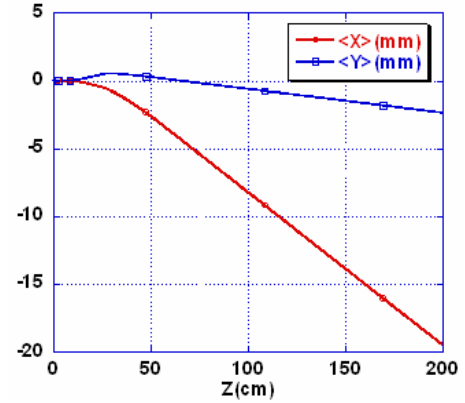


Figure 5: PARMELA computed X-Y centroids motion due to the dipolar components superimposed to the solenoid field

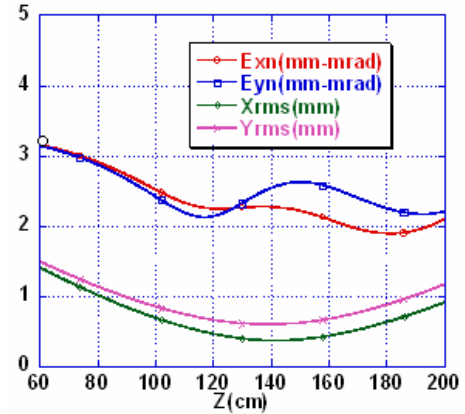


Figure 6: PARMELA computed rms X-Y envelopes and transverse normalized emittance vs z with only quadrupolar components superimposed to the solenoid field

This last effect is mainly due to the quadrupole-induced coupling of x - y planes.

In fact when a bunch passes through a skew quadrupole, even if the 4D emittance remains invariant, there is a change in the projected x - y emittances due to the coupling of the two planes induced by the quadrupole itself. The same effect occurs if the quadrupole (skew or not) is superimposed to a solenoidal magnetic field that rotates the bunch. As a consequence, even in the ideal case of a bunch passing through a hard edge solenoid with inside a quadrupole thin lens, the projected emittances vary. We can call this a ‘geometrical’ effect: the 4D

emittance remains invariant and the effect is reversible. For example, by using the matrix formalism, we evaluate analytically the bunch transverse dimensions after passing through a hard edge solenoid of length L_1+L_2 with a thin lens skew quadrupole at a position L_1 . If the bunch enters the system with zero emittances and σ_x and σ_y transverse dimensions, at the exit the transverse emittances are

$$\varepsilon_x^2 = \varepsilon_y^2 = \frac{\sigma_x^2 \sigma_y^2}{f^2} \cos^4(kL_1) \cos^2(kL_2) \quad (3)$$

with f the quadrupole focal length and k the Larmor wave number of the solenoid. If we substitute in the equation the typical values obtained for SPARC ($f=10\text{m}$, $\sigma_x=\sigma_y=1.5\text{mm}$, $\gamma=10$), the maximum value of the emittance is $\varepsilon_{nx}=\varepsilon_{ny}=2.25\text{mm mrad}$ that is very close to that obtained with PARMELA code.

A more detailed analysis based on the formalism of the classical evolution operators is reported in [3]. This analysis shows that it is the described geometrical effect the most important contribution to the quadrupole induced emittance growth, while the space charge acts almost independently. This result is confirmed in figure 7 where we plotted the 4D transverse matrix determinant obtained with PARMELA code (that includes the space charge), with and without a skew thin lens quadrupole superimposed to the solenoidal magnetic field. As can be seen, the two curves almost coincide well beyond the exit of the solenoidal field (at about 40 cm). As a consequence the observed emittance growth is actually due to geometrical projection of the 4D invariant along the x - y planes.

One important conclusion is that the emittance growth can be almost totally compensated by using one or more rotated quadrupoles since it is mainly due to geometrical projection of the 4D determinant. These quadrupoles can be placed immediately out of the solenoid before that the space charge introduces other correlations during the beam evolution in the post-gun drift region.

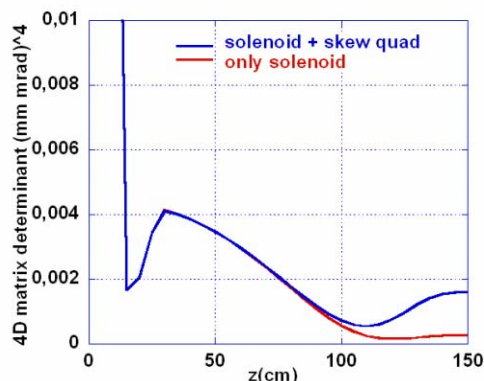


Figure 7: 4D transverse matrix determinant as a function of the longitudinal coordinate, obtained with PARMELA code with and without a skew thin lens quadrupole superimposed to the solenoid.

EXPERIMENTAL TESTS

The SPARC solenoid uses four different coils that can be powered by different power supply. Taking advantage

of this particular capability, three different options were tested, whose main characteristics in terms of excitation current, rotation angle and steering current are reported in Table 1.

Table 1. Different solenoid configurations.

| | Current signs | Current Value | Larmor angle* | Horizontal steering | Vertical Steering |
|---|---------------|---------------|---------------|---------------------|-------------------|
| A | ++++ | 125 A | 58.8° | 3 A | -11 A |
| B | ---- | 125 A | -58.8° | -2 A | 15 A |
| C | --++ | 200 A | 0° | 4 A | 1 A |

* $\pm 1.5^\circ$

The value of the current is chosen in order to keep constant the solenoid focusing power and is different between the configurations A,B and the configuration C due to the fact that the magnetic field cancels out (going to zero in the middle of the solenoid) when the coils are not powered with the same sign of current.

The angle of Larmor rotation was measured moving the laser beam on the cathode along horizontal and vertical directions and recording the directions of movement respectively of the electron beam on a target screen located 1.2 m downstream of the cathode.

The last two columns show for the three configurations the different setting of the current on the steering magnet located downstream of the solenoid: the configuration A requires the maximum correction due to the foreseen strong dipolar component superimposed to the solenoid field. A drastic reduction in the steering strength is achieved in the configuration C, where the dipole kicks are applied with different signs and cancel out. Another advantage of configuration C (which on the other hand requires a higher current in the coils) is that the Larmor angle is zero and the horizontal and vertical axes are preserved throughout the system. This simplifies the alignment procedure between the axis of the gun and of the solenoid and allows to study the effects of the ellipticity and/or uniformity of the laser beam on the cathode without recurring to image rotation filters.

As to the effect of the foreseen quadrupolar component: the experimental measurements are not yet conclusive to separate its effect from other sources of beam spot shape deformation and quality degradation (multipoles in the RF gun, misalignments in the compensation system of the laser oblique incidence, beam non uniformities...).

We plan to use more extensively the ability to change the larmor rotation angle independently from the focusing power of the solenoid in order to investigate the different effects.

REFERENCES

- [1] L. Serafini, "Status of the SPARC Project", this conference.
- [2] Y. Papaphilippou et al. "Deflection in magnet fringe fields"
- [3] F. Ciocci, et at., "Generalized Twiss Coefficients Including Transverse Coupling and E-beam Growth", this conference.